A Novel Therapeutic Approach to Treating Obesity through Modulation of TGF β Signaling

Alan Koncarevic, Shingo Kajimura, Milton Cornwall-Brady, Amy Andreucci, Abigail Pullen, Dianne Sako, Ravindra Kumar, Asya V. Grinberg, Katia Liharska, Jeffrey A. Ucran, Elizabeth Howard, Bruce M. Spiegelman, Jasbir Seehra, and Jennifer Lachey

Acceleron Pharma, Inc. Preclinical Pharmacology (A.K., M.C-B., A.P., J.S. and J.L.) and Bioanalytical Development and Cell Biology (A.A., D.S., R.K., A.V.G., K.L., J.A.U. and E.H.), Cambridge, Massachusetts 02139; University of California, San Francisco, Diabetes Center and Department of Cell and Tissue Biology (S.K.), University of California, San Francisco, San Francisco 94143; and Department of Cell Biology (B.M.S.), Harvard Medical School, and Dana-Farber Cancer Institute, Boston, Massachusetts 02115

Obesity results from disproportionately high energy intake relative to energy expenditure. Many therapeutic strategies have focused on the intake side of the equation, including pharmaceutical targeting of appetite and digestion. An alternative approach is to increase energy expenditure through physical activity or adaptive thermogenesis. A pharmacological way to increase muscle mass and hence exercise capacity is through inhibition of the activin receptor type IIB (ActRIIB). Muscle mass and strength is regulated, at least in part, by growth factors that signal via ActRIIB. Administration of a soluble ActRIIB protein comprised of a form of the extracellular domain of ActRIIB fused to a human Fc (ActRIIB-Fc) results in a substantial muscle mass increase in normal mice. However, ActRIIB is also present on and mediates the action of growth factors in adipose tissue, although the function of this system is poorly understood. In the current study, we report the effect of ActRIIB-Fc to suppress diet-induced obesity and linked metabolic dysfunctions in mice fed a high-fat diet. ActRIIB-Fc induced a brown fat-like thermogenic gene program in epididymal white fat, as shown by robustly increased expression of the thermogenic genes uncoupling protein 1 and peroxisomal proliferator-activated receptor- γ coactivator 1α . Finally, we identified multiple ligands capable of reducing thermogenesis that represent likely target ligands for the ActRIIB-Fc effects on the white fat depots. These data demonstrate that novel therapeutic ActRIIB-Fc improves obesity and obesity-linked metabolic disease by both increasing skeletal muscle mass and by inducing a gene program of thermogenesis in the white adipose tissues. (Endocrinology 153: 3133-3146, 2012)

Obesity is a worldwide epidemic and is driving increases in the development of type 2 diabetes, cardiovascular disease, and certain cancers. Compelling research demonstrates that even moderate weight loss can provide significant protection from cardiovascular disease and type 2 diabetes (1–4). Traditional obesity treatments

are aimed at preventing further accumulation of chemical energy in the form of fat by reducing appetite or nutrient uptake; however, treatments that positively affect peripheral energy use still offers great promise. For example, alterations in body composition to increase muscle mass could, in the absence of increased food intake, reduce ad-

ISSN Print 0013-7227 ISSN Online 1945-7170
Printed in U.S.A.
Copyright © 2012 by The Endocrine Society
doi: 10.1210/en.2012-1016 Received January 5, 2012. Accepted April 4, 2012.
First Published Online May 1, 2012

For editorial see page 2939

Abbreviations: ActRIIB, Activin receptor type IIB; ActRIIB-mFc, chimeric ActRIIB derivative; BAT, brown adipose tissue; BMP, bone morphogenetic protein; CT, computed tomography; DIO, diet-induced obesity; ECD, extracellular domain; FOXO1, Forkhead box O1; GDF, growth and differentiation factor; HDL, high-density lipoprotein; HFD, high-fat diet; HMW, high-molecular-weight; LDL, low-density lipoprotein; NMR, Nuclear magnetic resonance; PGC-1, peroxisomal proliferator-activated receptor- γ coactivator 1; RER, respiratory exchange ratio; Sirt, sirtuin; SPR, surface plasmon resonance; TBS, Tris-buffered saline; UCP1, uncoupling protein 1; VO2, O2 consumption; WAT, white adipose tissue.

iposity and help reduce the risk of obesity-related cardiovascular and metabolic diseases. Brown adipocytes are of special interest in that they have the ability to decrease obesity through thermogenesis mediated by uncoupling protein 1 (UCP1) (5–7). It has recently been shown that there are two types of brown fat that have distinctly different origins. The classical brown fat depots typified by the interscapular depot in mice arises from a common precursor with skeletal muscle (8). Brown fat-like cells (also called brite cells or beige cells) can also appear in white fat depots when an animal is exposed to β 3-adrenergic agonists or prolonged cold temperatures. Brown fat cells of both types are certainly novel and appealing targets for the development of antiobesity therapeutics (9).

Multiple members of the growth and differentiation factor (GDF) family, including myostatin (GDF-8), signal through activin receptor type IIB (ActRIIB) (10-13). These factors have been shown to negatively regulate muscle mass (14, 15) and may also be involved in the regulation of adipose tissue mass (16–18). Previous research in rodents demonstrates that inhibition of ActRIIB signaling with a chimeric ActRIIB derivative (ActRIIB-mFc), consisting of the extracellular domain of murine ActRIIB fused to a murine IgG2a Fc domain, results in greatly increased muscle mass in healthy mice (14), mice with amyotrophic lateral sclerosis (19), and mice exposed to a hypoxic environment (20). In addition, inhibition of ActRIIB signaling using a soluble receptor approach protected mice fed a high-fat diet (HFD) from developing diet-induced obesity (DIO) (18, 21, 22). The reduced susceptibility of mice with diminished ActRIIB signaling to DIO has been mainly attributed to inhibition of myostatin signaling and secondary to increased muscle (17, 18, 22). Importantly, ActRIIB is a signaling receptor for TGF β ligands other than myostatin, many that are expressed in adipose tissue and may also be targets for the soluble ActRIIB-driven effect of protection from DIO (23–27, 48).

We have developed the novel, human therapeutic ActRIIB-Fc to inhibit ActRIIB signaling. This soluble ActRIIB-Fc is comprised of a form of the ActRIIB extracellular domain fused to a human IgG Fc domain and acts as a soluble, decoy receptor to the endogenous ActRIIB. HFD feeding in mice results in adverse changes in body composition and metabolic parameters similar to those reported in obese human subjects. Therefore, we investigated the effects of ActRIIB-Fc on muscle mass, adiposity, and adiposity-related systemic physiological changes, such as changes in circulating concentrations of lipids and adipokines as well as lipid accumulation in liver and brown adipose tissue in mice fed a HFD. In this paper we report striking effects of this novel therapeutic on preventing obesity induced in mice by HFD. This reagent induces

many changes in the gene expression pattern of adipose tissues, including the induction of a brown fat-like gene program in the white fat, and these changes correlate with an increase in whole body energy expenditure. We also characterize ligands of the TGF β superfamily that regulate thermogenesis in primary adipocyte cultures and identify ligands that are potentially targeted by ActRIIB-Fc to elicit its effect on white fat.

Materials and Methods

Construction, expression, and purification of ActRIIB-human IgG1a Fc (ActRIIB-Fc)

The plasmid encodes the fusion molecule containing an optimized human activin receptor IIB extracellular domain (ECD; residues 24–131) followed by the human IgG1 Fc domain. The DNA sequence of the ECD was designed from human ActRIIB (synthesized by Blue Heron Biotechnology, Bothell, WA). The purified PCR fragment and the pAID4T vector were ligated to create the expression vector, in which the ActRIIB ECD was fused in-frame to the human IgG1 Fc domain. The complete cDNA sequence was confirmed by double-strand dideoxy sequencing (Sequegen Co., Worcester, MA). The construct was transiently transfected into human embryonic kidney 293 cells. After 1 wk of growth at 37 C, the conditioned media were harvested with a two-step column chromatography procedure. The purified ActRIIB-Fc was eluted from the column and then dialyzed into Tris-buffered saline (TBS).

Animals and experimental design

Twenty-four 10-wk-old, male C57BL/6 (Taconic, Germantown, NY) mice were weighed, individually numbered, and assigned to weight-matched treatment groups. All procedures were reviewed and approved by Acceleron Pharma, Inc. Animal Care and Use Committee (Cambridge, MA). All animals were housed in conventional cages under a 12-h dark, 12-h light cycle at a constant temperature of 17 C and relative humidity maintained between 30 and 40% with free access to water and either regular chow diet (Chow; Purina LabDiet 5001; St. Louis, MO) or HFD (Research Diets D12331; New Brunswick, NJ). Mice fed a HFD were dosed sc twice weekly with ActRIIB-Fc (designated HFD plus ActRIIB-Fc; 10 mg/kg, n = 8) or vehicle (designated HFD; body weight volume modified TBS, n = 7) for a period of 60 d. Animals fed a normal diet (designated Chow) were dosed with TBS (n = 7) for the same duration. Mice within the same treatment cohort were housed together in groups of three or four. Upon termination of the study, the mice were euthanized by CO_2 .

Body and terminal tissue weights

Body weights were measured twice per week at the time of administration of TBS or ActRIIB-Fc. At the study termination date, tissues of interest (blood, muscles, brown adipose tissue depot, epididymal fat depots) were surgically removed, weighed, and properly stored for further analysis.

Nuclear magnetic resonance (NMR)

Body composition was analyzed at d 0 (before administration of ActRIB-Fc and transfer to HFD) and then again at d 27 and 48 of the 60-d study using the MiniSpec LF90 NMR analyzer (Bruker, Woodlands, TX).

In vivo assessment of abdominal adipose tissue content and brown adipose tissue density by micro-computed tomography (CT)

Micro-CT imaging was performed in anesthetized mice using a vivaCT 75 small-angle-cone-beam micro-CT imaging system (Scanco Medical AG, Bassersdorf, Switzerland) with resolution of 20.5–156 μm nominal (pixel size). Methods for the analysis of abdominal adipose tissue and thigh muscle adipose tissue content are previously described (28). Brown adipose tissue content was measured using approximately 300 transverse CT slices ranging from thoracic vertebrae T1 to T6 were acquired by using 41-μm isotropic voxel size (45 kVp, 177 μA, 1024 samples at 1000 projections per 360°, 350 msec integration time). Images were reconstructed and filtered, and a threshold segmenting brown adipose from other tissue was applied.

Enzyme-linked immunosorbent assays

Upon study termination, the mice were euthanized using CO_2 and blood was collected into serum separation tubes. After a 10-min centrifugation at $10,000 \times g$, serum was collected and used for subsequent immunoassays according to manufacturer instructions. The total and high-molecular-weight adiponectin ELISA was purchased from ALPCO Immunoassays (Salem, NH), leptin ELISA from Crystal Chem (Downers Grove, IL), and insulin ELISA from Linco Research (St. Charles, MO).

Serum lipid analysis

Serum samples were sent to AniLytics Inc. (Gaithersburg, MD) for enzymatic measurement of triglycerides, nonesterified free fatty acids, high-density lipoproteins (HDL), and low-density lipoproteins (LDL).

Histology and immunohistochemistry

Upon study termination, white adipose tissue depots, brown adipose tissue depots, and livers were surgically dissected and processed as follows. Adipose tissue depots were fixed overnight in 10% formalin and stored in 70% ethanol. The fixed adipose depots were then paraffin embedded, sectioned into 10-μm sections, and processed for hematoxylin and eosin stain. Dissected livers were snap frozen in liquid nitrogen, sectioned into 10-μm sections, and processed for Oil Red O stain. Immunohistochemistry for UCP1 protein was performed on deparaffinized epididymal fat sections using anti-UCP1 primary antibody (Abcam 10983, 1:500 dilution, Cambridge, MA), followed by incubation with an antirabbit Alexa-488 secondary antibody, and mounting in 4′,6′-diamino-2-phenylindole containing mounting medium. All images of the stained sections were taken using a camera connected to a fluorescence-capable light microscope.

Gene expression analysis

Total RNA was isolated from frozen epididymal fat depots and a two-step RT-PCR analysis was performed for quantitation of mRNA levels of *UCP1*, peroxisomal proliferator-activated receptor- γ coactivator 1 (*PGC-1*)- α , *cidea*, sirtuin (*Sirt*)-1, Forkhead box O1 (*FOXO1*), *GDF-3*, and *GDF-8*. The RT-PCR was performed using the following TaqMan Gene expression assays from Applied Biosystems (Foster City, CA): Mm01244862_m1 (*UCP1*), Mm00447181_m1 (*PGC-1* α), Mm00432554_m1 (*cidea*), Mm01168521_m1 (*Sirt-1*), and Mm00490672_m1 (*FOXO1*). All assays were normalized to 18S mRNA expression, which was used as an internal control.

Energy expenditure

Thirty 13-wk-old, male C57BL/6 mice (Taconic) were weighed, individually numbered, and assigned to weightmatched treatment groups. HFD-fed mice were further subdivided into one of two treatment groups: ActRIIB mFc, a murine form of ActRIIB-Fc comprised of the same extracellular domain as in ActRIIB-Fc, but the Fc is murine rather than human (10 mg/kg, n = 10) or vehicle (designated HFD; body weight volume modified TBS, n = 10). Chow-fed mice (designated Chow) were dosed with TBS (n = 10). All groups received twice-weekly injections for 60 d of treatment before being transported to the Mouse Phenotyping Core (Baylor College of Medicine, Houston, TX) for calorimetric analysis. Indirect calorimetry was performed using an open-circuit oxymax chamber, a component of the comprehensive laboratory animal monitoring system (Columbus Instruments, Columbus, OH). Analysis was performed as previously described (29) with the exception that in our study, the mice did not have an acclimation period. Briefly, mice were placed into individual metabolic chambers with ad libitum access to food and water. Twenty-four-hour food intake measurements were taken across study d 63 and 64. O₂ consumption (VO₂) and CO₂ production were measured and respiratory exchange ratio (RER; ratio of VO₂ to CO₂ production) was determined at 10min intervals for a 24-h period on study d 63-64.

Cell culture experiments in primary mouse adipocytes

The stromal-vascular fraction was isolated from the inguinal adipose tissue of C57BL/6 male mice (Taconic). The cells were cultured to confluence and differentiated for 2 d in differentiation medium containing 10 µg/ml insulin (Sigma, St. Louis, MO), 100 ng/ml T₃ (Sigma), 1 μM rosiglitazone (Cayman Chemical, Ann Arbor, MI), 0.125 mm indomethacin (Sigma), 4 μg/ml dexamethasone (Sigma), and 0.5 mm 3-isobutyl-1-methylxanthine (Sigma). Subsequently the stromal-vascular cells were cultured in maintenance medium containing 10 ng/ml insulin, 100 ng/ml T_3 , and 1 μ M rosiglitazone. These cells were treated with TGFβ ligands at 100 ng/ml for 3 d. For the ActRIIB-Fc cotreatment studies, adipocytes were treated with 1 μg/ml ActRIIB-Fc 1 h before ligand treatment was initiated. Cells were cultured in the presence of both ActRIIB-Fc and ligand for an additional 3 d. Recombinant bone morphogenetic protein (BMP)-2, BMP-4, BMP-7, GDF-5, GDF-6, GDF-7, GDF-8, GDF-9, GDF-11, and activin B proteins were purchased from R&D Systems (Minneapolis, MN). GDF-3 and activin A were made at Acceleron Pharma. All samples were performed in triplicate. RNA was extracted and quantitative RT-PCR was performed using SYBR green (Applied Biosystems). All the values were normalized by TATA box binding protein. Primer sequences have been previously published (30).

ActRIB-Fc ligand binding determination using surface plasmon resonance (SPR)

Biacore T100, research grade CM5 chips, and amine coupling reagents were purchased from Biacore (GE Healthcare, Indianapolis, IN). Activin A, GDF-11, and GDF-3 were produced at Acceleron Pharma. GDF-8 was obtained from Fitzgerald Industries (Concord, MA). Other ligands were obtained from R&D systems. Receptor-ligand binding affinities were determined by SPR using Biacore T100. Goat antihuman Fc antibody was immobilized onto four flow cells of research-grade CM5 chip using standard amino-coupling chemistry. ActRIIB-Fc was captured on the experimental flow cells. Another flow cell was used as a reference (control) to subtract for nonspecific binding, drift, and bulk refractive index. For kinetic analysis, a concentration series of different ligands were injected over experimental and control flow cells at 20 or 25 C at a flow rate of 40 µl/min or greater to minimize mass transport limitations. The antibody surface was regenerated between binding cycles by injection of 10 mm glycine (pH 1.7). A buffer of 0.01 M HEPES, 0.5 M NaCl, 3 mm EDTA, 0.005% (vol/vol) surfactant P20 (pH 7.4) containing 0.5 mg/ml BSA was used as a running buffer. All sensograms were processed by double referencing. To obtain kinetic rate constants, the corrected data were fitted to 1:1 interaction model with mass transport term using BiaEvaluation software (Biacore). The equilibrium dissociation constant was determined as the ratio of the dissociation to the association rate constants.

Data analysis

Comparisons between treatment groups over time (longitudinal) were made using ANOVA followed by least squares-mean differences Tukey honestly significant difference *post hoc* analysis. Comparisons between groups at a single time point (cross) were made using one-way ANOVA Tukey honestly significant difference pair test. Differences were considered statistically significant when the two-tailed $P \leq 0.05$. All data were analyzed with JMP 8.0 software (SAS Institute, Inc., Cary, NC). Data shown are means \pm SEM.

Results

ActRIIB-Fc increases lean tissue mass and prevents adipose tissue mass gain in mice fed a HFD

We first investigated the effects of ActRIIB-Fc on body composition in mice fed a HFD, an animal model that mimics many of the changes in body composition and metabolic parameters seen in obese humans. As shown in Fig. 1A, mice fed the HFD, with or without ActRIIB-Fc, showed an increase in body mass relative to the chow-fed mice. Despite the excessive weight gain in both of these groups, the HFD and HFD plus ActRIIB-Fc treatments had dramatically different effects on body composition. HFD plus ActRIIB-Fc treatment resulted in a marked gain in lean tissue (49.8%; Fig. 1B) compared with both the chow and HFD groups. ActRIIB-Fc also altered fat mass gain (Fig. 1C). As expected, mice on the HFD gained substantially more fat mass compared with chow-fed mice

(Fig. 1C). In contrast, the amount of fat gained in the HFD plus ActRIIB-Fc-treated mice was greatly reduced compared with HFD receiving vehicle.

We confirmed the whole-body NMR data with micro-CT imaging. Images of the abdominal sc and visceral adipose depots illustrated the increase in visceral and sc depots resulting from the HFD compared with chow. In comparison, the visceral and sc depots from HFD plus ActRIIB-Fc were 64 and 58% smaller, respectively (Fig. 1, D and E). In addition, representative images of a midthigh region obtained by micro-CT illustrate a reduction in intramuscular fat in the ActRIIB-Fc group and depict the similarity of body composition in mice on HFD treated with ActRIIB-Fc to that in chow-fed controls (Fig. 1F). Finally, the HFD and HFD plus ActRIIB-Fc groups had comparable 24-h food intake, supporting the idea that ActRIIB-Fc effect on body composition is not simply the result of an ActRIIB-Fc-mediated hypophagia (Fig. 1G).

ActRIIB-Fc prevents HFD-induced alterations in serum hormones and lipids in addition to preventing inappropriate lipid accumulation in liver and brown fat

In addition to assessing the effect of ActRIIB-Fc on HFD-induced adiposity, we determined its effects on HFD-related alterations to circulating hormones, serum lipids, and triglyceride accumulation in liver and brown fat. HFD reduced the contribution of high-molecularweight (HMW) adiponectin to total adiponectin levels by 89.5% compared with the chow-fed group (Fig. 2A). In contrast, ActRIIB-Fc prevented the HFD-induced alteration and in fact maintained the ratio of HMW adiponectin to those of chow-fed mice (Fig. 2A). As expected, HFD feeding also resulted in increased circulating serum leptin and insulin levels compared with the chow controls (Fig. 2, B and C). Consistent with the reduced adiposity in the ActRIIB-Fc group, the levels of circulating leptin and insulin were reduced compared with the HFD group (*P* < 0.05, Fig. 2, B and C). Obesity is associated with increased circulating serum lipid content. In this study, 60 d of the HFD resulted in a 90.9% increase in serum free fatty acids, a 131.4% increase in serum triglycerides, and a 106.0% increase in HDL compared with chow-fed mice. ActRIIB-Fc treatment completely prevented the HFD-related changes in all three parameters, such that the levels were not significantly different from the chow group (Fig. 2, D-F). Additionally, the LDL was increased in response to the HFD feeding, and, although this effect was not completely abolished in the ActRIIB-Fc group, ActRIIB-Fc treatment was able to significantly attenuate this rise (Fig. 2G).

In addition to elevating lipid levels in circulation, HFD also results in inappropriate deposition of lipid in the liver.

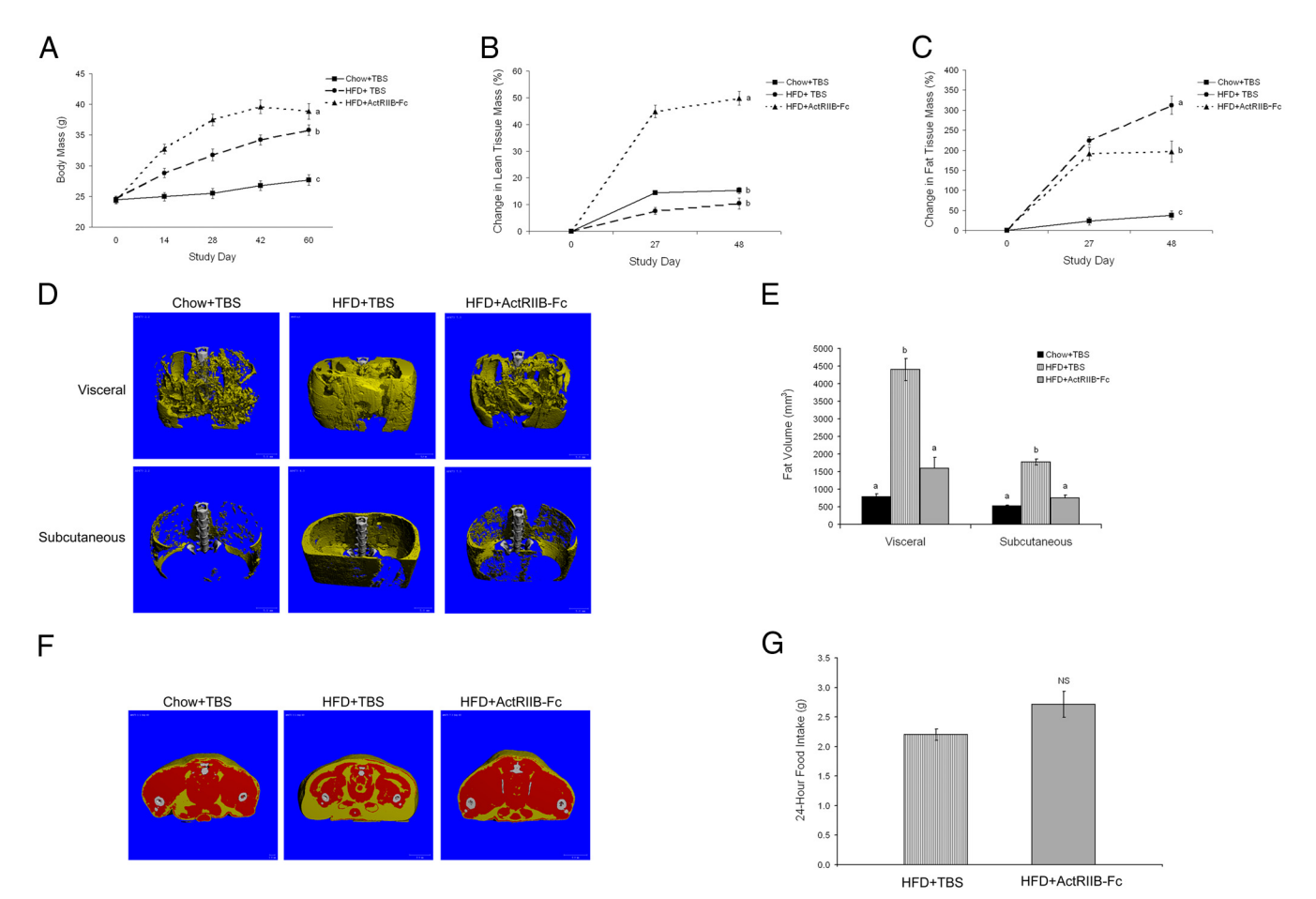


FIG. 1. A, Body weight over time in mice as a function of HFD and ActRIIB-Fc treatment. Vehicle was TBS. Data shown are means (n=10 per group), and d 60 means that differ significantly (P < 0.05) are designated by *different letters*. B, Percent change in lean tissue mass over time in mice as a function of HFD and ActRIIB-Fc treatment. Measurements were made by NMR, data shown are means (n=10 per group), and means that differ significantly (P < 0.05) are designated by *different letters*. C, Percent change in fat tissue mass over time in mice as a function of HFD and ActRIIB-Fc treatment. Measurements were made by NMR, data shown are means (n=10 per group), and means that differ significantly (P < 0.05) are designated by *different letters*. D, Abdominal fat (visceral and sc) in mice as a function of 60 d of HFD and ActRIIB-Fc treatment. Representative three-dimensional micro-CT images show fat (*yellow*) and bone (*white*). E, Quantitative analysis of visceral and sc abdominal fat volume in mice as a function of 60 d of HFD and ActRIIB-Fc treatment. Seven mice from each experimental group were randomly selected and the abdominal fat was quantified using micro-CT imaging. Data shown are means (n=7 per group), and means that differ significantly (P < 0.05) are designated by *different letters*. F, Tissue composition in mice as a function of 60 d of HFD and ActRIIB-Fc treatment. Representative micro-CT images of transverse sections at the midthigh level indicate muscle (*red*), fat (*yellow*), and bone (*white*). G, Food consumption of mice fed a HFD and treated with either TBS or ActRIIB-Fc for 60 d. Data shown are means (n=8 per group), NS, Not significantly different from HFD-fed group treated with TBS.

Liver triglyceride content, as visualized by Oil Red O staining, was increased in mice on HFD compared with mice on chow (Fig. 2H), consistent with liver steatosis (*i.e.* fatty liver). This lipid-accumulating effect of HFD was prevented in mice treated with ActRIIB-Fc as seen by fewer Oil Red O-stained lipid droplets (Fig. 2H).

It has been previously reported that HFD feeding in mice results in increased interscapular brown adipose tissue (BAT) mass and adipocyte hypertrophy (31–33) as a result of increased lipid accumulation in the tissue. As expected, in our current study, we found that 60 d of HFD feeding increased the overall BAT size (Fig. 3A) and nearly doubled BAT mass (Fig. 3B). ActRIIB-Fc completely prevented the effect of HFD feeding on both BAT size and

mass (Figs. 3, A and B). Furthermore, we used micro-CT imaging and histology to assess the effects of HFD feeding on BAT density and found that HFD in mice fed HFD, the density of the BAT is measurably reduced. We further validated this finding histologically in which we visualized the increased lipid storage (Fig. 3E) in the adipocytes. The HFD-induced change in the BAT lipid accumulation was completely prevented by ActRIB-Fc in terms of both BAT density and lipid content of the tissue (Fig. 3, C–E). Additionally, the percentage that BAT mass contributes to total body weight differs across diet and treatment groups. BAT weight increased at a greater rate than the total mouse body weight in the HFD-fed group. The disproportionately high increase in BAT mass is consistent with

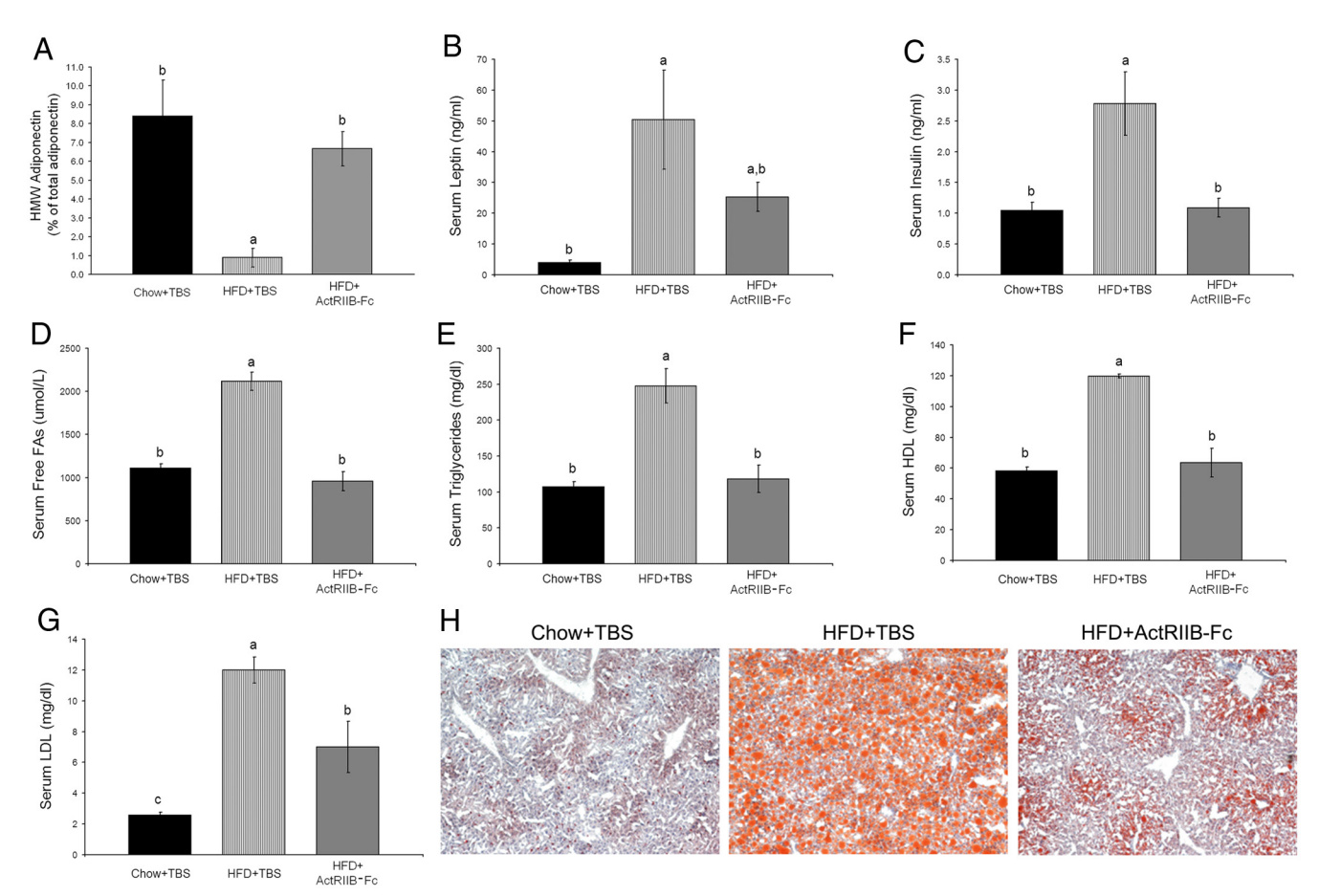


FIG. 2. A, Percent HMW of total serum adiponectin concentrations in mice as a function of HFD and ActRIIB-Fc treatment for 60 d. B, Serum leptin concentrations in mice as a function of HFD and ActRIIB-Fc treatment for 60 d. C, Serum insulin concentrations in mice as a function of HFD and ActRIIB-Fc treatment for 60 d. D, Serum concentrations of free fatty acids in mice as a function of HFD and ActRIIB-Fc treatment for 60 d. E, Serum concentrations of triglycerides in mice as a function of HFD and ActRIIB-Fc treatment for 60 d. F, Serum concentrations of HDL in mice as a function of HFD and ActRIIB-Fc treatment for 60 d. G, Serum concentrations of LDL in mice as a function of HFD and ActRIIB-Fc treatment for 60 d. Data shown are means \pm SEM (n = 10 per group), and those that differ significantly (P < 0.05) are designated by different letters. H, Liver triglyceride content as a function of HFD and ActRIIB-Fc treatment for 60 d. Liver sections were hematoxylin and eosin stained and visualized using light microscopy. Magnification, \times 20.

it being a target tissue for ectopic fat deposition in a setting of excess calories (Supplemental Fig. 1, published on The Endocrine Society's Journals Online web site at http://endo.endojournals.org). In contrast, BAT mass in ActRIIB-Fc-treated mice remains constant despite significant body weight gain so the percentage of BAT weight represented in the total body weight is smaller compared with vehicle treated mice on either chow or HFD. This finding suggests that ActRIIB-Fc mediates its effect on muscle independently from its effect on BAT and that BAT mass is not indirectly affected by muscle hypertrophy.

ActRIIB-Fc protection from diet-induced obesity results from increased energy expenditure and not decreased caloric intake

ActRIIB-Fc treatment provided protection from the increased adiposity and adiposity-related changes that result from a HFD without affecting food intake. To confirm

that the ActRIIB-Fc-mediated protection from DIO was largely driven by increased energy expenditure, we conducted an indirect calorimetry study. For this set of studies, we used a slightly modified version of the ActRIIB. It was engineered with a mouse rather than a human Fc domain whereas the extracellular, active portion of the protein was completely unchanged (human amino acid sequence for both molecules). We have previously determined that both compounds have equivalent effects on body composition and DIO protection (data not shown). HFD plus ActRIIB-Fc-treated mice had 30% higher energy consumption than the HFD counterparts, supporting the idea that ActRIIB-Fc treatment prevents obesity by increasing energy expenditure and not by affecting food intake (Fig. 4, A and B). Additionally, there was a change in the RER between the groups. ActRIIB-Fc-treated mice had a tendency to preferentially use carbohydrate sub-

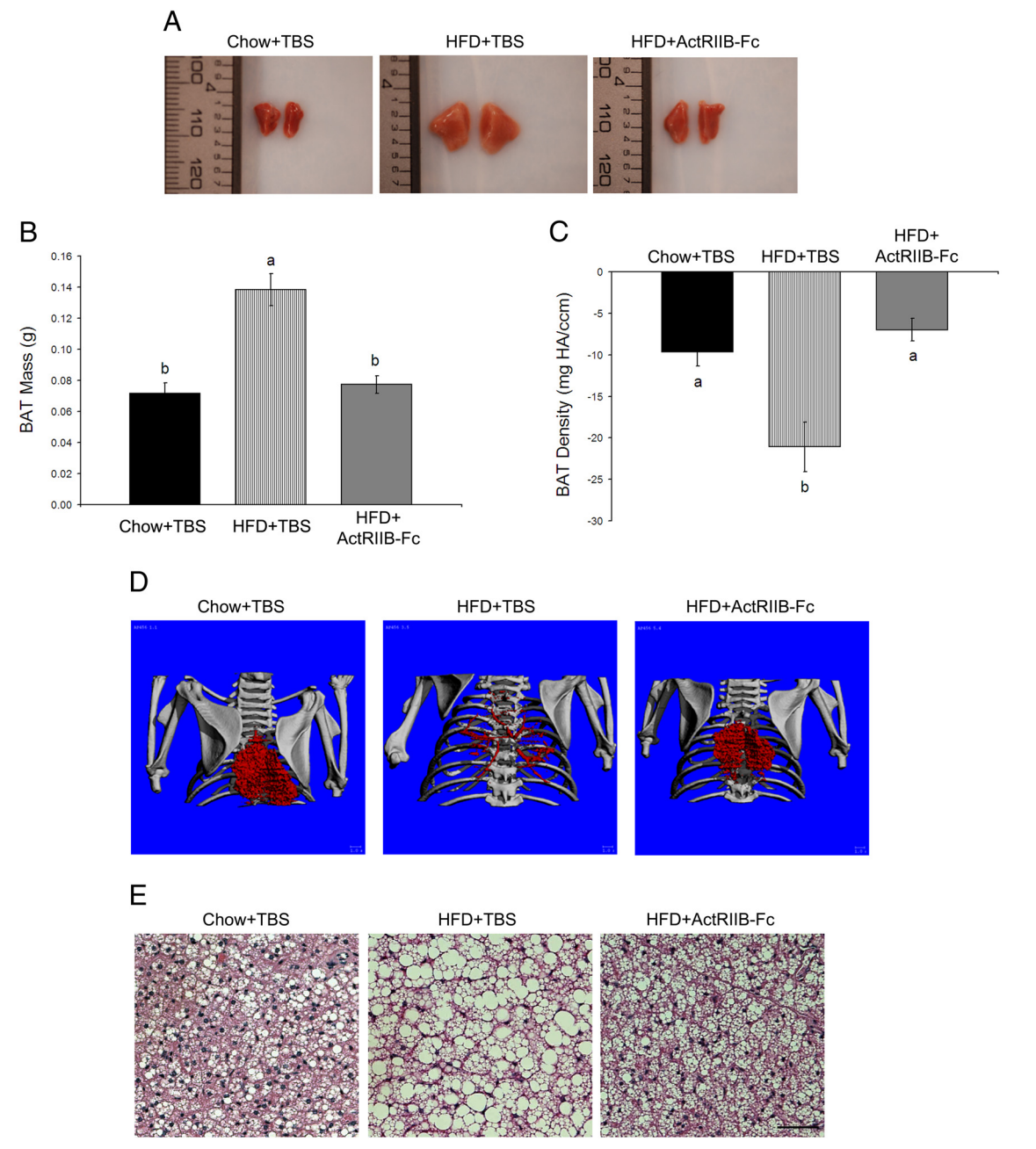


FIG. 3. A, Digital photographs of representative interscapular BAT depots dissected from mice after 60 d of HFD and ActRIB-Fc treatment. B, BAT mass as a function of 60 d of HFD and ActRIB-Fc treatment. Data shown are means (n=10 per group), and means that differ significantly (P < 0.05) are designated by *different letters*. C, Quantitative analysis of BAT density in mice as a function of 60 d of HFD and ActRIB-Fc treatment. Seven mice from each experimental group were randomly selected, and the BAT density was quantified using micro-CT imaging. Data shown are means (n=7 per group), and means that differ significantly (P < 0.05) are designated by *different letters*. D, BAT in mice as a function of 60 d of HFD and ActRIB-Fc treatment. Representative three-dimensional micro-CT images show BAT (red) and bone (white). E, BAT triglyceride content as a function of HFD and ActRIB-Fc treatment for 60 d. BAT sections were hematoxylin and eosin stained and visualized using light microscopy. Magnification, $\times 20$ ($large\ pane$).

strates (Fig. 4, C and D), although whether this affected lipid utilization is unknown.

ActRIIB-Fc increases expression of thermogenesis genes in white fat tissue

Previous literature supports a role for ActRIIB signaling in regulating white adipose tissue and in mediating

changes that occur in fat depots in response to HFD feeding (17). Additionally, specific ActRIIB-Fc target ligands have been implicated in adipogenesis (26, 34) as well as the control of mitochondrial biogenesis in white adipose tissue (26, 35). In addition to the classical BAT in the interscapular region, emergence of newly recruited brown fat-like cells in white adipose tissue (WAT) appears to be

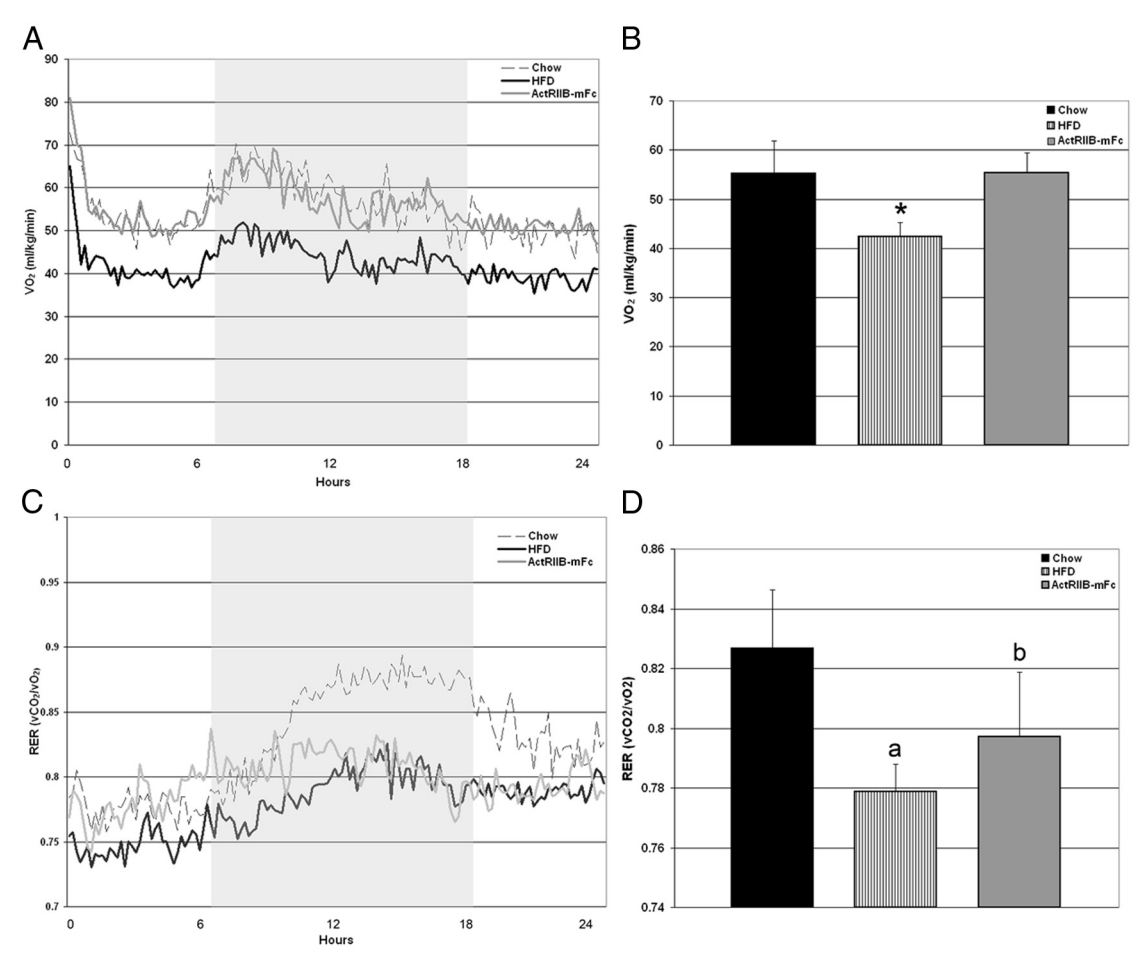


FIG. 4. A, Oxygen consumption tracings from chow (dotted gray line), HFD (solid black line), and ActRIIB-mFc (solid gray line) groups. B, Mean VO_2 consumption over the 24-h measurement period was significantly lower in the HFD group (gray bar) compared with that of the chow (white bar) and ActRIIB-mFc (black bar) cohorts (P < 0.001; n = 8/group). C, Representative RER tracing from chow (dotted gray line), HFD (solid black line), and ActRIIB mFc (solid gray line) groups. B, The ActRIIB-mFc (black bar) cohort had significantly higher RER measurements compared with HFD (gray bar; P < 0.05; n = 8/group), but both had lower RER compared with that of chow (white bar). B and D, Means that are significantly different are designated by different letters.

important target for the antiobesity therapeutics (6, 8, 9). Hence, we studied whether ActRIIB-Fc inhibition of ActRIIB signaling induces the brown fat-like cells in the epididymal WAT by measuring several brown fat-enriched genes such as UCP1, $PGC-1\alpha$, and cidea. Strikingly, HFD plus ActRIIB-Fc treatment resulted in an approximately 60-fold up-regulation of gene expression for UCP1, an approximately 1.5-fold increase in cidea, and a 3.5-fold induction of $PGC-1\alpha$ compared with the HFD groups (Fig. 5, A–C). Importantly, this ActRIIB-Fc-driven effect extends beyond the level of gene expression. When we assayed the epidydimal fat pads for changes in UCP1 protein, we found pockets of multilocular, UCP1-positive areas in the ActRIIB-Fc samples, whereas there was negligible UCP1 immunoreactivity in the HFD WAT. Histologically we confirmed that these regions had the multilocular appearance also characteristic of brown fat. These data demonstrate that ActRIIB-Fc treatment is not simply changing the transcriptome of WAT but that the WAT is producing the key brown fat proteins. In addition, *FOXO1* was up-regulated and there was a trend for *Sirt-1* up-regulation, further supporting fat use rather than storage occurring in HFD plus ActRIIB-Fc-treated mice (Supplemental Fig. 2). We did not detect statistically significant changes in gene expression or protein levels of PRDM16, which may be a matter of the time point from which the tissue was assayed or further support that thermogenesis in epididymal fat is not under PRDM16 regulation (36).

Ligands in the TGF β superfamily differentially regulate thermogenic gene expression in primary white adipocytes, and ActRIIB-Fc inhibits multiple ligands, which negatively regulate thermogenesis

ActRIB-Fc treatment increases expression of thermogenic genes in WAT, and presumably this effect is the result of the soluble receptor binding and inactivating ligands that would otherwise act to repress thermogenesis. To determine which $TGF\beta$ ligands able to bind to Ac-

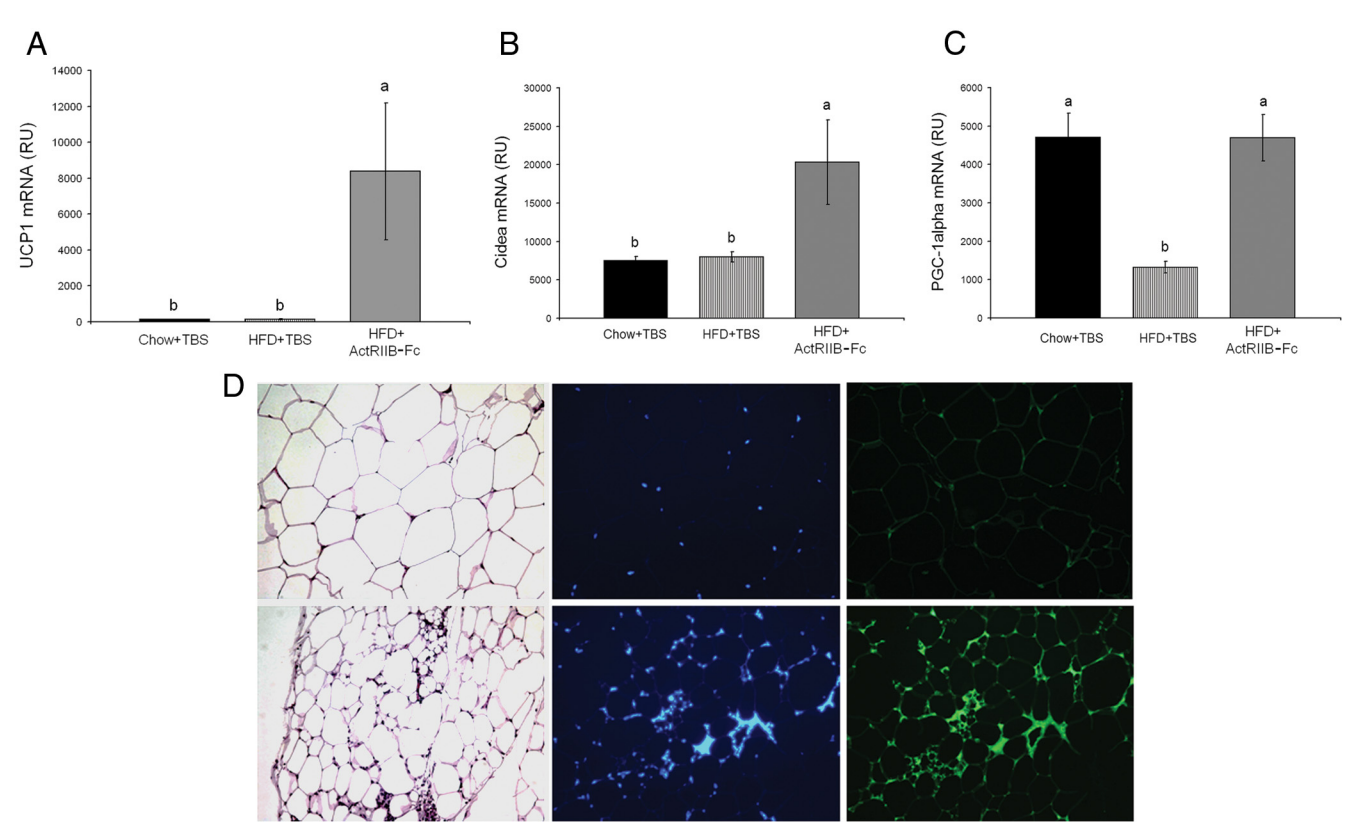


FIG. 5. Relative expression of thermogenic genes in epididymal WAT of mice as a function of 60 d of HFD and ActRIB-Fc treatment. Quantitative real-time PCR was used to assess relative gene expression of UCP1 (A), cidea (B), and PGC-1 α (C). 18S mRNA expression was used as an internal control for all of the evaluated genes. Data shown are means (n = 10 per group), and means that differ significantly (P < 0.05) are designated by different letters. D, Hematoxylin and eosin stain of formalin-fixed, paraffin-embedded sections of epididymal WAT from mice fed a HFD and treated with either TBS (top left) or ActRIB-Fc (bottom left) for 60 d visualized with light microscopy (×10). 4',6'-diamino-2-phenylindole-stained nuclei in epididymal WAT from mice treated with either TBS (top center) or ActRIB-Fc (bottom center) visualized with fluorescence microscopy (×10). UCP1 protein expression in tissue sections of epididymal WAT from mice fed a HFD and treated with either TBS (top right) or ActRIB-Fc (bottom right) for 60 d visualized using fluorescence microscopy (×10).

tRIIB-Fc, we first conducted the SPR assay. The SPR screening identified GDF-3, GDF-8, GDF-11, activin A, and activin B as high-affinity ligands for ActRIIB-Fc. GDF-5, GDF-6, GDF-7, and BMP-7 were intermediate binders, and BMP-2 and BMP-4 were low binders. GDF-9 was identified as a nonbinding ligand (Fig. 6A). Next, we screened for which TGF β ligands inhibited expression of thermogenic genes using primary cultured white adipocytes. As shown in Fig. 6B, UCP1 gene expression was significantly down-regulated after treatment with the ActRIIB-Fc high-affinity ligands (GDF-3, GDF-8, GDF-9, GDF-11, and activins A and B) as well as the nonbinder GDF-9. ActRIIB also binds BMP-9 and BMP-10, but these ligands did not produce any changes in UCP1 in the primary white fat cultures and therefore were not further characterized (data not shown) (13). The intermediate binders GDF-5, GDF-7, and BMP-7 significantly up-regulated UCP1 expression in the cultured adipocytes as did the low-affinity BMP-2 and BMP-4 (Fig. 6B). Although the effect on UCP1 expression was the most dramatic, we found the similar trend for the additional brown fat-spe-

cific markers *cidea* and $PGC-1\alpha$ in which high-affinity binders had the greatest effect on suppressing expression, whereas the intermediate and low binders actually increased expression levels (Fig. 6, C and D). The effect of the inhibitory ligands on the specific markers for brown fat UCP1 and cidea was maintained after normalization to the expression of the adipocyte fatty acid binding protein ap2, indicating that the down-regulation is not merely the result of overall inhibition of adipogenesis (Supplemental Fig. 3). Additionally, we determined the ability of ActRIIB-Fc to inhibit the UCP1 down-regulation mediated by ActRIIB high-affinity ligands in vitro. Culturing adipocytes with the high-affinity ligands (GDF-8, GDF-11, and activins A and B) in the presence of ActRIIB-Fc either fully restored or made significant improvements to the UCP1 expression. In this study, GDF-3 did not have a measurable effect on UCP1 expression, and we found no change when combined with ActRIIB-Fc treatment. As a negative control, we tested the effect of cotreatment with ActRIIB-Fc and the non-ActRIIB binder GDF-9. GDF-9 markedly inhibited UCP1 expression and ActRIIB-Fc was Α

Analysis of ActRIIB-Fc binding to different ligands by SPR

Ligand	ka (M-1s-1)	k d (s-1)	K _D (M)	Liga
Activin A	1.03 x 10 ⁷	2.20 x 10 ⁻⁴	2.14 x 10 ⁻¹¹	вмі
Activin B	6.18 x 10 ⁶	3.38 x 10 ⁻⁵	5.46 x 10 ⁻¹²	вмі
GDF11	3.56×10^6	2.52 x 10 ⁻⁵	7.07×10^{-12}	GDF
GDF8	3.62 x 10 ⁵	4.05 x 10 ⁻⁵	1.12 x 10 ⁻¹⁰	GDF
GDF3	2.14 x 10 ⁵	5.06 x 10 ⁻⁴	2.37 x 10 ⁻⁹	mGD
BMP2			2.47 x 10 ⁻⁸ **	mGD

Ligand	ka (M-1s-1)	k d (s-1)	$K_{\mathbf{D}}$ (M)		
BMP4			>1.27 x 10 ⁻⁷ **		
BMP7	1.20 x 10 ⁷	1.01×10^{-2}	10 ⁻² 8.45 x 10 ⁻¹⁰		
GDF5	6.50 x 10 ⁶	9.8 x 10 ⁻³	1.50 x 10 ⁻⁹		
GDF6	1.31 x 10 ⁶	1.26×10^{-2}	9.58 x 10 ⁻⁹		
mGDF7	2.47×10^{7}	10 ⁷ 9.9 x 10 ⁻³ 3.99 x			
mGDF9	No binding*				

^{***}K_D obtained by steady state affinity fit, due to the very fast association and dissociation of the complex, which prevents accurate k_a and k_d measurements.

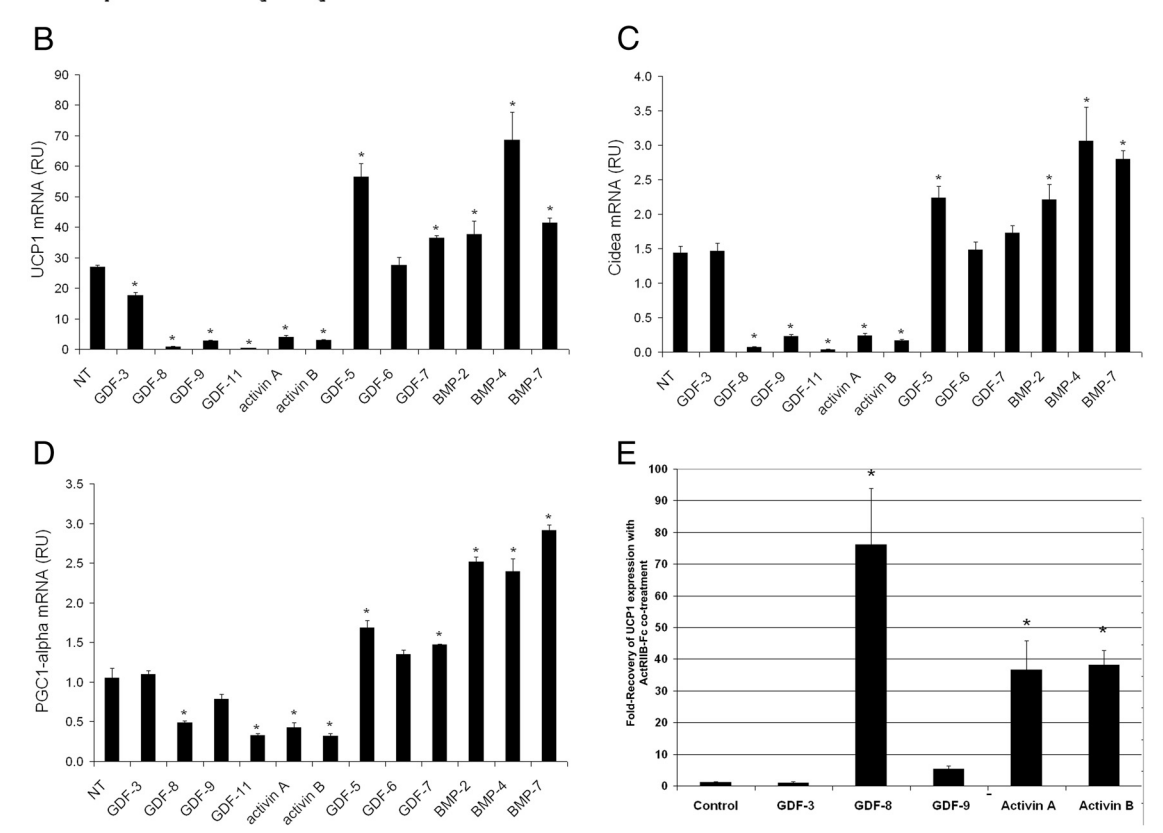


FIG. 6. A, Analysis of ActRIIB-Fc binding to different ligands by SPR. Purified ActRIIB-Fc was captured on a Biacore sensor chip by immobilized antihuman Fc antibody; different concentrations of ligands were injected over captured receptor in duplicates. Kinetic analysis was performed with Biacore T100 at 25C except for BMP-2, which was performed at 20C. Data were globally fit to a 1:1 binding model with mass transfer term using BIAevaluation software (Biacore). B–D, Expression of thermogenic genes in cultured, differentiated, primary adipocytes from WAT in response to treatments with select TGF β members. UCP1 (B), cidea (C), and PGC-1 α (D) mRNA expression levels as a function of treatment with GDF-3, GDF-8, GDF-9, GDF-11, activin A, and activin B ligands. E, Expression of UCP1 in cultured, differentiated, primary adipocytes from WAT in response to treatment with select TGF β members with or without the addition of ActRIIB-Fc. Quantitative real-time PCR was used to assess relative expression of the genes of interest using TATA box binding protein mRNA expression as an internal control. Data shown are means (n = 3 per group). κ a, Association rate constant; κ d, dissociation rate constant; κ D, equilibrium dissociation constant; NT, no treatment. *, P < 0.05.

ineffective at preventing this effect (Fig. 6E). Taken together, these data support that ActRIIB-Fc binds with high affinity to the negative regulators of thermogenesis (*i.e.* the high affinity ligands) and consequently permits an emergence of brown fat-like cells in WAT. Importantly, this effect occurs without impeding the effects of the ligands that ordinarily may act to drive thermogenesis in WAT (the intermediate and low affinity binders). All together these data support that ActRIIB-Fc-treated mice increase

their energy expenditure sufficiently to offset the increased energy load from HFD feeding rather than succumb to DIO and its associated consequences.

Discussion

These studies demonstrate the efficacy of the therapeutic ActRIIB-Fc in offsetting the effects of HFD feeding and

^{*} No binding at 100 nM

identify two mechanisms that could be driving the ActRIIB-Fc-mediated increase in energy expenditure. First, ActRIIB-Fc treatment resulted in nearly a 40% increase in overall lean mass compared with the untreated HFD-fed mice. Multiple TGF β ligands, the best characterized being GDF-8 (myostatin), act via the ActRIIB to negatively regulate muscle mass growth. ActRIIB-Fc, being a form of soluble ActRIIB, binds these ligands with high affinity and prevents their signaling at the endogenous receptor, which results in increased muscle mass. Previous work provides a more detailed description of the effect on muscle, but in summary, ActRIIB-Fc treatment increases myofiber size of both oxidative and glycolytic fibers without affecting fiber number or fiber type distribution (20, 21, 37). Second, ActRIIB-Fc treatment robustly induced a number of brown fat-like thermogenic genes, including UCP1 and $PGC-1\alpha$ in pockets of WAT. Considerable numbers of brown adipocytes occur transiently within some white fat depots during early postnatal development (38) and can reappear in white fat depots under certain conditions in adulthood (39). Even in humans, limited evidence suggests that brown adipocytes are inducible in white fat depots during adulthood (40). The molecular signals that regulate this process are not fully understood; however, our data support a role for ActRIIB signaling. Importantly, our results strongly suggest that induced brown fat-like adipocytes interspersed within WAT significantly contribute to the regulation of whole-body energy metabolism. Indeed, it has been reported that mouse strains with enhanced capacity to induce UCP1 expression and brown adipocyte differentiation in white fat lost weight at a higher rate in response to adrenergic stimulation than the strains that with lower UCP1 induction potential (41).

Interestingly, the ActRIIB-Fc increase in muscle mass occurs ahead of its effect of reducing fat mass gain. Lean mass is significantly increased by ActRIIB-Fc treatment at the first time point (d 27) and continues to be increased at d 48, whereas the fat mass in the vehicle and ActRIIB-Fc HFD groups do not diverge until d 48. One possibility for the adiposity effect lagging behind the effect on muscle is that the increased muscle is contributing to the protection from DIO. Increasing muscle is an effective means to offset excess calories, and although this effect is likely a key contributor to the overall effect, we propose that the change in fat phenotype also plays an independent role from the muscle. Certain TGF β ligands, including GDF-3, are expressed in WAT and their expression levels increase with HFD feeding (25–27, 42, 48). In the case of GDF-3, overexpression of the ligand is associated with an increased level of obesity, whereas genetic ablation prevents DIO (27, 48). Importantly, the nature of the protection from DIO was identified as being an up-regulation of thermogenesis in WAT with no change in muscle mass. Therefore, targeting GDF-3 and/or other ligands with a similar function is sufficient to offset the effects of HF feeding, so it is likely that the ActRIIB-Fc effect on WAT is contributing to the net effect of prevention of DIO. Again, the levels of these ActRIIB-Fc ligands are low in lean animals but increase as obesity progresses, so it is possible that the lag in the ActRIIB-Fc direct effect on WAT requires these changes in the properties of the WAT.

Future studies will address the specific contribution of muscle and fat tissues to the overall effect of DIO protection. In addition, we will more closely consider the possible contributions of additional organ systems. For example, our studies determined that the ActRIIB-Fc effect on HFD feeding is not due to hypophagia, but based on the data from our studies, we cannot rule out the possibility that there is a difference in nutrient absorption between the groups that could be contributing to the reduced adiposity in the ActRIIB-Fc treatment group.

In using a mouse model to understand the effects of a molecule derived from human sequence, it is important to consider the possibility of the formation of neutralizing antibodies against the drug itself for the interpretation of the study. In our case, the extracellular domains of the human and mouse ActRIIB are highly homologous and differ only by a single amino acid; therefore, it is unlikely that neutralizing antibodies would be formed against the extracellular binding region of the drug. Consistent with this, the muscle mass increase characteristic of myostatin inhibition as well as the protection against DIO was consistently maintained across the duration of the study. Antibodies against the Fc portion would not be expected to interfere with the binding of the drug to its target ligands, but to test for this unlikely event, we ran studies with molecules having the same ActRIIB extracellular domain but with either a human or a mouse Fc. These two molecules had comparable effects on body weight and body composition, which supports the idea that if there are antibodies directed against the Fc portion of the human molecule, they do not interfere with the pharmacological effects of the molecule. These data support that the effects reported are drug specific and are not altered by antidrug antibody production.

Members of the TGF β superfamily act to control differentiation of a multiple tissue types, including fat. Previous work has characterized a substantial TGF β superfamily regulation of the thermogenic potential of white fat. TGF β 1, through SMAD signaling, reduces markers of mitochondrial biogenesis in white fat (43). In addition to TGF β , genetic deletion of myostatin as well as inhibition of ActRIIB promotes a brown fat phenotype in white fat depots (18). We confirm the finding of Zhang *et al.* (18) of

increased thermogenesis genes in white fat after the administration of ActRIIB-Fc, although the UCP1 levels of the chow-fed groups differ between our study and theirs and the magnitude of UCP1 effect in response to treatment is also different. We find a low basal level of UCP1 in both the chow and HFD groups, whereas the study by Zhang et al. describes a HFD-induced decrease in UCP1 compared with chow-fed mice. In their study, UCP1 levels are restored to that of the chow group, whereas we report a 60-fold up-regulation with ActRIB-Fc treatment. This difference could be due to the properties of our soluble receptor constructs or possibly to the differences in dose and duration of treatment. However, in addition to myostatin, other ligands in the TGF β superfamily have been implicated in the regulation of WAT and may be acting through the ActRIIB (25–27, 42, 48).

To better understand the role these ligands play in white fat, we first assessed their effect on regulating expression of thermogenic factors in white fat primary cultures. In this set of studies, activing A and B and GDF-3, GDF-8, and GDF-11 were characterized as UCP1 and PGC-1α inhibitors. We also identified these ligands as being highaffinity ActRIIB ligands, and therefore, ActRIIB-Fc may be having its effects on white fat through inhibition of these factors. In addition, we assayed the UCP1 and $PGC-1\alpha$ response to GDF-5, GDF-6, and GDF-7 and BMP-2, BMP-4, and BMP-7. The thermogenesis phenotype was increased in response to these factors. These ligands were also found to bind to ActRIIB with intermediate to low affinity and are therefore not directly affected by ActRIIB-Fc treatment. It is possible the ActRIIB-Fc is indirectly influencing the ability of the prothermogenesis factors to signal by sequestering the negative regulators, which ordinarily compete for the downstream signaling machinery. Little is known about the role of GDF-9 outside oocyte development (44). We found it reduced UCP1 expression, but the SPR data confirmed it as a non-ActRIIB binder, so it is mediating its effects independently of the ActRIIB. Taken together, these data suggest that the effect of ActRIIB-Fc on increasing a brown fat phenotype in white fat may be mediated not only by directly by inhibiting ActRIIB signaling but also by sequestering the negative regulators, permitting greater signaling from the pro-thermogenesis ligands.

We identified GDF-8, GDF-11, activin A, activin B, and GDF-3 as potential mediators of the described ActRIIB-Fc effects in WAT. Consistent with this finding, previous work has described the expression of ActRIIB and certain of its high-affinity ligands in white fat (17, 23, 25, 26, 35). For example, GDF-3 and GDF-8 are expressed in white adipose tissue, are up-regulated in response to HFD, and, given our data demonstrating their suppression of *UCP1*,

may be acting to promote the storage rather than the burning of fat. Therefore, inhibition of these ligands may be a suitable strategy for the management of obesity. Activins A and B are also expressed in white fat, although they might localize to different cell populations (23, 25, 35, 45). Similar to GDF-3 and GDF-8, expression of activins A and B are thought to positively associate with metabolic disease (25, 45, 46) and are therefore possible targets for the treatment of obesity. ActRIIB-Fc is a soluble form of the ActRIIB, a receptor common to all of these ligands, and we demonstrate its inhibition of these ligands. The ability of ActRIIB-Fc to inhibit the multiple negative regulators is a feature that presumably would result in a broader inhibition of the negative regulators and provide a more maximal effect on UCP1 up-regulation compared with targeting the ligands individually.

Interestingly, McPherron et al. (47) have reported that treatment with a soluble ActRIIB did not decrease adiposity in mice with established DIO. In their paper, mice were fed a HFD for 12 wk and maintained on this diet during 12 wk of treatment with a soluble ActRIIB. The treatment schedule was a dose of 10 mg/kg · wk for 4 wk followed by an additional 8 wk of 5 mg/kg·wk. This dosage significantly increased muscle mass in the DIO mice but offered no protection from continued fat mass accumulation. In this study, the effect of converting white fat to a brown fat phenotype was not assessed. Therefore, it is not clear whether the treatment failed to increase thermogenesis in white fat at all or whether the effect on white fat occurred but was insufficient to offset the preexisting adiposity under continued HFD feeding. Given that our results support a prevention of DIO when treatment with 10 mg/kg twice weekly is given concomitant to HFD, future work will need to address possible differences in the browning effect mediated by different dosages of soluble ActRIIB and explore the effect of the TGFB superfamily members in regulating adipose tissue from obese mice.

These findings identify a novel potential mechanism for induction of thermogenic profile in predominantly WAT and provide grounds for the use of ActRIB-Fc in treatment of obesity and obesity-related metabolic disorders.

Acknowledgments

We thank Dr. Monique Davies, Dr. Kathryn Underwood, Dr. Kathleen Tomkinson, June Liu, Rashel Burton, Theresa Baker, Ben Umiker, Travis Monnell, Joseph Barberio, and Matthew Spaits for all of their efforts in construct design, protein purification, and pharmacology support. We also express our thanks to the Mouse Phenotyping Core (Baylor College of Medicine, Houston, TX) for their help in coordinating and running the

comprehensive laboratory animal monitoring system studies. All studies were funded by Acceleron Pharma.

Address all correspondence and requests for reprints to: Jennifer Lachey, 128 Sidney Street, Cambridge, Massachusetts 02139. E-mail: jlachey@acceleronpharma.com.

Disclosure Summary: A.K., M.C.-B., A.A., A.P., D.S., R.K., A.V.G., K.L., J.A.U., E.H., J.S. and J.L. have been compensated by Acceleron Pharma, Inc. B.M.S. and S.K. are consultants to Acceleron Pharma. B.M.S. is a founder and shareholder of Ember Therapeutics, Inc.

References

- National Institutes of Health 1998 Clinical guidelines on the identification, evaluation, and treatment of overweight and obesity in adults—the evidence report. Obes Res 6(Suppl 2):51S–209S
- 2002 Evidence-based nutrition principles and recommendations for the treatment and prevention of diabetes and related complications. Diabetes Care 25:202–212
- Goldstein DJ 1992 Beneficial health effects of modest weight loss. Int J Obes Relat Metab Disord 16:397–415
- Wing RR, Koeske R, Epstein LH, Nowalk MP, Gooding W, Becker D 1987 Long-term effects of modest weight loss in type II diabetic patients. Arch Intern Med 147:1749–1753
- Frontini A, Cinti S 2010 Distribution and development of brown adipocytes in the murine and human adipose organ. Cell Metab 11:253–256
- Kajimura S, Seale P, Spiegelman BM 2010 Transcriptional control of brown fat development. Cell Metab 11:257–262
- 7. Nedergaard J, Cannon B 2010 The changed metabolic world with human brown adipose tissue: therapeutic visions. Cell Metab 11: 268–277
- 8. Seale P, Bjork B, Yang W, Kajimura S, Chin S, Kuang S, Scimè A, Devarakonda S, Conroe HM, Erdjument-Bromage H, Tempst P, Rudnicki MA, Beier DR, Spiegelman BM 2008 PRDM16 controls a brown fat/skeletal muscle switch. Nature 454:961–967
- Cypess AM, Kahn CR 2010 Brown fat as a therapy for obesity and diabetes. Curr Opin Endocrinol Diabetes Obes 17:143–149
- Attisano L, Wrana JL, Cheifetz S, Massagué J 1992 Novel activin receptors: distinct genes and alternative mRNA splicing generate a repertoire of serine/threonine kinase receptors. Cell 68:97–108
- Mathews LS, Vale WW 1991 Expression cloning of an activin receptor, a predicted transmembrane serine kinase. Cell 65:973–982
- 12. Sako D, Grinberg AV, Liu J, Davies MV, Castonguay R, Maniatis S, Andreucci AJ, Pobre EG, Tomkinson KN, Monnell TE, Ucran JA, Martinez-Hackert E, Pearsall RS, Underwood KW, Seehra J, Kumar R 2010 Characterization of the ligand binding functionality of the extracellular domain of activin receptor type IIb. J Biol Chem 285: 21037–21048
- 13. Souza TA, Chen X, Guo Y, Sava P, Zhang J, Hill JJ, Yaworsky PJ, Qiu Y 2008 Proteomic identification and functional validation of activins and bone morphogenetic protein 11 as candidate novel muscle mass regulators. Mol Endocrinol 22:2689–2702
- 14. Lee SJ, Reed LA, Davies MV, Girgenrath S, Goad ME, Tomkinson KN, Wright JF, Barker C, Ehrmantraut G, Holmstrom J, Trowell B, Gertz B, Jiang MS, Sebald SM, Matzuk M, Li E, Liang LF, Quattlebaum E, Stotish RL, Wolfman NM 2005 Regulation of muscle growth by multiple ligands signaling through activin type II receptors. Proc Natl Acad Sci USA 102:18117–18122
- Lee SJ, Lee YS, Zimmers TA, Soleimani A, Matzuk MM, Tsuchida K, Cohn RD, Barton ER 2010 Regulation of muscle mass by follistatin and activins. Mol Endocrinol 24:1998–2008

- McPherron AC, Lee SJ 2002 Suppression of body fat accumulation in myostatin-deficient mice. J Clin Invest 109:595–601
- 17. Allen DL, Cleary AS, Speaker KJ, Lindsay SF, Uyenishi J, Reed JM, Madden MC, Mehan RS 2008 Myostatin, activin receptor IIb, and follistatin-like-3 gene expression are altered in adipose tissue and skeletal muscle of obese mice. Am J Physiol Endocrinol Metab 294: E918–E927
- 18. Zhang C, McFarlane C, Lokireddy S, Masuda S, Ge X, Gluckman PD, Sharma M, Kambadur R 2012 Inhibition of myostatin protects against diet-induced obesity by enhancing fatty acid oxidation and promoting a brown adipose phenotype in mice. Diabetologia 55: 183–193
- Morrison BM, Lachey JL, Warsing LC, Ting BL, Pullen AE, Underwood KW, Kumar R, Sako D, Grinberg A, Wong V, Colantuoni E, Seehra JS, Wagner KR 2009 A soluble activin type IIB receptor improves function in a mouse model of amyotrophic lateral sclerosis. Exp Neurol 217:258–268
- Pistilli EE, Bogdanovich S, Mosqueira M, Lachey J, Seehra J, Khurana TS 2010 Pretreatment with a soluble activin type IIB receptor/Fc fusion protein improves hypoxia-induced muscle dysfunction. Am J Physiol Regul Integr Comp Physiol 298:R96–R103
- Akpan I, Goncalves MD, Dhir R, Yin X, Pistilli EE, Bogdanovich S, Khurana TS, Ucran J, Lachey J, Ahima RS 2009 The effects of a soluble activin type IIB receptor on obesity and insulin sensitivity. Int J Obes (Lond) 33:1265–1273
- 22. Guo T, Jou W, Chanturiya T, Portas J, Gavrilova O, McPherron AC 2009 Myostatin inhibition in muscle, but not adipose tissue, decreases fat mass and improves insulin sensitivity. PLoS One 4:e4937
- 23. Hoggard N, Cruickshank M, Moar KM, Barrett P, Bashir S, Miller JD 2009 Inhibin βB expression in murine adipose tissue and its regulation by leptin, insulin and dexamethasone. J Mol Endocrinol 43:171–177
- 24. McPherron AC, Lee SJ 1993 GDF-3 and GDF-9: two new members of the transforming growth factor-beta superfamily containing a novel pattern of cysteines. J Biol Chem 268:3444–3449
- 25. Zaragosi LE, Wdziekonski B, Villageois P, Keophiphath M, Maumus M, Tchkonia T, Bourlier V, Mohsen-Kanson T, Ladoux A, Elabd C, Scheideler M, Trajanoski Z, Takashima Y, Amri EZ, Lacasa D, Sengenes C, Ailhaud G, Clément K, Bouloumie A, Kirkland JL, Dani C 2010 Activin A plays a critical role in proliferation and differentiation of human adipose progenitors. Diabetes 59: 2513–2521
- Wang W, Yang Y, Meng Y, Shi Y 2004 GDF-3 is an adipogenic cytokine under high fat dietary condition. Biochem Biophys Res Commun 321:1024–1031
- Shen JJ, Huang L, Li L, Jorgez C, Matzuk MM, Brown CW 2009
 Deficiency of growth differentiation factor 3 protects against diet-induced obesity by selectively acting on white adipose. Mol Endocrinol 23:113–123
- 28. Koncarevic A, Cornwall-Brady M, Pullen A, Davies M, Sako D, Liu J, Kumar R, Tomkinson K, Baker T, Umiker B, Monnell T, Grinberg AV, Liharska K, Underwood KW, Ucran JA, Howard E, Barberio J, Spaits M, Pearsall S, Seehra J, Lachey J 2010 A soluble activin receptor type IIb prevents the effects of androgen deprivation on body composition and bone health. Endocrinology 151:4289–4300
- Kennedy AR, Pissios P, Otu H, Roberson R, Xue B, Asakura K, Furukawa N, Marino FE, Liu FF, Kahn BB, Libermann TA, Maratos-Flier E 2007 A high-fat, ketogenic diet induces a unique metabolic state in mice. Am J Physiol Endocrinol Metab 292:E1724

 E1739
- Kajimura S, Seale P, Kubota K, Lunsford E, Frangioni JV, Gygi SP, Spiegelman BM 2009 Initiation of myoblast to brown fat switch by a PRDM16-C/EBP-β transcriptional complex. Nature 460:1154– 1158
- 31. Herberg L, Döppen W, Major E, Gries FA 1974 Dietary-induced hypertrophic-hyperplastic obesity in mice. J Lipid Res 15:580–585
- 32. Jo J, Gavrilova O, Pack S, Jou W, Mullen S, Sumner AE, Cushman

- SW, Periwal V 2009 Hypertrophy and/or hyperplasia: dynamics of adipose tissue growth. PLoS Comput Biol 5:e1000324
- Mercer SW, Trayhurn P 1987 Effect of high fat diets on energy balance and thermogenesis in brown adipose tissue of lean and genetically obese ob/ob mice. J Nutr 117:2147–2153
- 34. Artaza JN, Bhasin S, Magee TR, Reisz-Porszasz S, Shen R, Groome NP, Meerasahib MF, Fareez MM, Gonzalez-Cadavid NF 2005 Myostatin inhibits myogenesis and promotes adipogenesis in C3H 10T(1/2) mesenchymal multipotent cells. Endocrinology 146:3547–3557
- Li L, Shen JJ, Bournat JC, Huang L, Chattopadhyay A, Li Z, Shaw C, Graham BH, Brown CW 2009 Activin signaling: effects on body composition and mitochondrial energy metabolism. Endocrinology 150:3521–3529
- Seale P, Conroe HM, Estall J, Kajimura S, Frontini A, Ishibashi J, Cohen P, Cinti S, Spiegelman BM 2011 Prdm16 determines the thermogenic program of subcutaneous white adipose tissue in mice. J Clin Invest 121:96–105
- 37. Cadena SM, Tomkinson KN, Monnell TE, Spaits MS, Kumar R, Underwood KW, Pearsall RS, Lachey JL 2010 Administration of a soluble activin type IIB receptor promotes skeletal muscle growth independent of fiber type. J Appl Physiol 109:635–642
- 38. Xue B, Rim JS, Hogan JC, Coulter AA, Koza RA, Kozak LP 2007 Genetic variability affects the development of brown adipocytes in white fat but not in interscapular brown fat. J Lipid Res 48:41–51
- Cousin B, Cinti S, Morroni M, Raimbault S, Ricquier D, Penicaud L, Casteilla L 1992 Occurrence of brown adipocytes in rat white adipose tissue: molecular and morphological characterization. J Cell Sci 103(Pt 4):931–942
- 40. Lean ME, James WP, Jennings G, Trayhurn P 1986 Brown adipose tissue in patients with phaeochromocytoma. Int J Obes 10:219–227

- 41. Guerra C, Koza RA, Yamashita H, Walsh K, Kozak LP 1998 Emergence of brown adipocytes in white fat in mice is under genetic control. Effects on body weight and adiposity. J Clin Invest 102: 412–420
- 42. Brown CW, Houston-Hawkins DE, Woodruff TK, Matzuk MM 2000 Insertion of Inhbb into the Inhba locus rescues the Inhba-null phenotype and reveals new activin functions. Nat Genet 25:453–457
- 43. Yadav H, Quijano C, Kamaraju AK, Gavrilova O, Malek R, Chen W, Zerfas P, Zhigang D, Wright EC, Stuelten C, Sun P, Lonning S, Skarulis M, Sumner AE, Finkel T, Rane SG 2011 Protection from obesity and diabetes by blockade of TGF-β/Smad3 signaling. Cell Metab 14:67–79
- 44. Gilchrist RB, Lane M, Thompson JG 2008 Oocyte-secreted factors: regulators of cumulus cell function and oocyte quality. Hum Reprod Update 14:159–177
- 45. Sjöholm K, Palming J, Lystig TC, Jennische E, Woodruff TK, Carlsson B, Carlsson LM 2006 The expression of inhibin βB is high in human adipocytes, reduced by weight loss, and correlates to factors implicated in metabolic disease. Biochem Biophys Res Commun 344:1308–1314
- 46. Carlsson LM, Jacobson P, Walley A, Froguel P, Sjöstrom L, Svensson PA, Sjöholm K 2009 ALK7 expression is specific for adipose tissue, reduced in obesity and correlates to factors implicated in metabolic disease. Biochem Biophys Res Commun 382:309–314
- 47. McPherron AC, Guo T, Wang Q, Portas J 2011 Soluble activin receptor type IIB treatment does not cause fat loss in mice with diet-induced obesity. Diabetes Obes Metab 14:279–282
- 48. Andersson O, Korach-Andre M, Reissmann E, Ibáñez CF, Bertolino P 2008 Growth/differentiation factor 3 signals through ALK7 and regulates accumulation of adipose tissue and diet-induced obesity. Proc Natl Acad Sci USA 105:7252–7256





Challenge your diagnostic skills with a one-of-a-kind self-assessment resource, *Diagnostic Dilemmas: Images in Endocrinology*, edited by Leonard Wartofsky, M.D.